

Properties of the solvation force of a two-dimensional Ising strip in scaling regimes

Piotr Nowakowski and Marek Napiórkowski

Institute of Theoretical Physics, University of Warsaw, Hoża 69, 00-681 Warszawa, Poland

E-mail: pionow@fuw.edu.pl

Abstract. We consider $d = 2$ Ising strip with surface fields acting on boundary spins. Using the properties of the transfer matrix spectrum we identify two pseudotransition temperatures and show that they satisfy similar scaling relations as expected for real transition temperatures in strips with $d > 2$. The solvation force between the boundaries of the strip is analysed as a function of temperature, surface fields and the width of the strip. For large widths the solvation force can be described by scaling functions in three different regimes: in the vicinity of the critical wetting temperature of 2D semi-infinite system, in the vicinity of the bulk critical temperature, and in the regime of weak surface fields where the critical wetting temperature tends towards the bulk critical temperature. The properties of the relevant scaling functions are discussed.

PACS numbers: 05.50.+q, 68.35.Rh, 68.08.Bc

1. Introduction

Fluctuating condensed-matter systems enclosed by walls are characterised by the appearance of solvation force acting between the walls. This force originates from the fluctuations of the confined system. The properties of solvation forces have been the subject of increasing interest during the last years [1, 2, 3, 4, 5, 6, 7, 8, 9, 10, 11, 12, 13, 14, 15, 16, 17, 18]. Both the shapes and possible chemical inhomogeneity of the confining walls influence the form of solvation forces [4, 6, 15, 16, 17] which additionally depend on the thermodynamic state of the system and on the interaction between the system and the walls. In particular, if the system is chosen to be at its bulk critical point the solvation forces become long ranged and show universality [19] while in the vicinity of criticality scaling behaviour is observed [20, 21].

In this article we analyse the solvation forces in two-dimensional Ising strips. The spins are confined by two parallel, planar and chemically homogeneous walls separated by distance M . Each wall interacts with the system by surface fields acting on the boundary spins. Our goal is the exact determination of the properties of the solvation forces as functions of temperature, surface fields and the width of the strip M . To

investigate these properties we use a method based on exact diagonalization of the transfer matrix which is followed by numerical determination of appropriate eigenvalues.

The paper is organised as follows. In section 2 we define the 2D Ising strip, recall its properties in the bulk limit as well as the properties of the semi-infinite system related to critical wetting. In section 3 we define pseudotransition temperatures and check that they display the scaling properties expected for higher dimensional systems. Section 4 is devoted to our main goal, i.e. analysis of the properties of the solvation force acting between the system boundaries. We first recall the definition of solvation force and adapt it to our model. We study this force numerically to establish several of its properties as functions of temperature, surface fields and the distance between the walls. For large width of the strip we explain these properties by introducing scaling functions in three different scaling regimes: around the wetting temperature, around the bulk critical temperature, and in regime in which both of the above temperatures are close to each other.

2. Ising strip

2.1. The model

We consider an Ising model on a two-dimensional square lattice with N columns and M rows, and impose periodic boundary conditions in the horizontal direction. In this way the Ising strip of width M is obtained. We assume that surface fields h_1 and h_2 act on the spins located at the bottom and the top row, respectively; these fields can be considered as model short range interactions between the system and the surrounding walls. The Hamiltonian of the system has the form

$$\mathcal{H}(\{s_{n,m}\}) = -J \sum_{n=1}^N \sum_{m=1}^{M-1} (s_{n,m}s_{n+1,m} + s_{n,m}s_{n,m+1}) - \sum_{n=1}^N (h_1 s_{n,1} + h_2 s_{n,M}), \quad (1)$$

where $s_{n,m} = \pm 1$ denotes the spin located in the n -th column and m -th row, and $s_{N+1,m} = s_{1,m}$. The coupling constant J is positive (ferromagnetic case) and we assume no bulk field h acting on the system.

In this paper, we concentrate on two special choices of surface fields corresponding to the so-called symmetric and antisymmetric case: in the symmetric case (denoted by the superscript S) one has $h_1 = h_2$ while in the antisymmetric case (AS) $h_1 = -h_2$. Later on, we will also use superscript O to denote the limiting case $h_1 = h_2 = 0$ which is referred to as the free case.

2.2. The free energy of the strip

To calculate the free energy of our system we use the method based on exact diagonalization of the transfer matrix. In this method the $2^{M+2} \times 2^{M+2}$ transfer matrix is represented by $(2M + 4) \times (2M + 4)$ orthogonal matrix R . Eigenvalues of the transfer matrix are calculated from eigenvalues of R which can be found by solving recurrence

equations for eigenvectors of R [22, 23, 24]. Here we only recall the final formulae for the free energy per column (here and in the following formulae we do not explicitly write the dependence of the free energy and other quantities on the coupling constant J)

$$\bar{f}^S(T, h_1, M) = -k_B T \left[\frac{1}{2} (\gamma_1 + \gamma_2 + \gamma_3 + \dots + \gamma_{M+1}) + \frac{M}{2} \ln(2 \sinh 2K) \right], \quad (2)$$

$$\bar{f}^{AS}(T, h_1, M) = -k_B T \left[\frac{1}{2} (-\gamma_1 + \gamma_2 + \gamma_3 + \dots + \gamma_{M+1}) + \frac{M}{2} \ln(2 \sinh 2K) \right], \quad (3)$$

where $K = J/k_B T$ and k_B is the Boltzmann constant. The coefficients $\gamma_1 < \gamma_2 < \dots < \gamma_{M+1}$ are positive functions of parameters T, h_1 and M defined by relation

$$\cosh \gamma_k = \cosh(2K - 2K^*) + 1 - \cos \omega_k, \quad (4)$$

where parameter K^* is obtained from $\sinh 2K \sinh 2K^* = 1$. The functions ω_k are solutions of the equations

$$(M+1)\omega_k - \delta'(\omega_k, T) - \phi(\omega_k, T, h_1) = (k-l)\pi, \quad 0 < \omega_k < \pi, \quad (5)$$

and $k = 1, 2, \dots, M+1$. The function $l(T, h_1)$ is defined as

$$l(T, h_1) = \begin{cases} 2 & \text{for } T < T_w, \\ 0 & \text{for } T_w < T < T_c, \\ 1 & \text{for } T > T_c. \end{cases} \quad (6)$$

The symbol T_c denotes the bulk critical temperature [25]

$$K_c = \frac{J}{k_B T_c} = \frac{1}{2} \ln(1 + \sqrt{2}), \quad (7)$$

while $T_w(h_1)$ denotes the temperature of the critical wetting transition taking place in the semi-infinite Ising model. It depends on the surface field h_1 and can be defined by equation [26]

$$W(T_w, h_1) = 1, \quad (8)$$

where

$$W(T, h_1) = (\cosh 2K^* + 1)(\cosh 2K - \cosh 2K_1), \quad K_1 = \frac{h_1}{k_B T}. \quad (9)$$

We observe that for certain ranges of temperatures (5) may not have a solution for $k = 1$ and $k = 2$. In such cases ω_1 and ω_2 are imaginary and satisfy equations

$$\omega_k = iu_k, \quad e^{-u_k M} = \alpha_k \exp\{i[\phi(iu_k, T) + \delta'(iu_k, T, h_1)]\}, \quad k = 1, 2, \quad (10)$$

with $\alpha_k = \pm 1$. The detailed rules for selecting the signs of α_1 and α_2 are presented in the next subsection. Functions ϕ and δ' are calculated from the formulae

$$e^{i\phi(\omega, T, h_1)} = e^{i\omega} \frac{W e^{i\omega} - 1}{e^{i\omega} - W}, \quad e^{2i\delta'(\omega, T)} = \frac{(e^{i\omega} - A)(e^{i\omega} - B)}{(A e^{i\omega} - 1)(B e^{i\omega} - 1)}, \quad (11)$$

where $A(T) = (\tanh K \tanh K^*)^{-1}$, $B(T) = \tanh K / \tanh K^*$, and the function $W(T, h_1)$ is given in (9). To determine the angles $\phi(\omega, T, h_1)$ and $\delta'(\omega, T)$ uniquely we pick the continuous branches of solutions for which

$$\phi(0, T, h_1) = \pi, \quad \delta'(0, T) = -\pi. \quad (12)$$

For $\omega = 0$ and $T = T_w$, the angle $\phi(\omega, T, h_1)$ is undefined ($W(T_w, h_1) = 1$) while at $T = T_c$ the angle $\delta'(\omega, T)$ is undefined ($K = K^*$, so $B = 1$). Although at these temperatures our formulae are useless one can use the continuity of the free energy and calculate it using a limiting procedure.

2.3. The characteristic temperatures

Because the lower critical dimension of the Ising model equals two ($d_l = 2$), no true transition may occur in a two-dimensional Ising strip with finite M . On the other hand, the infinite 2D Ising model experiences the critical point behaviour at $T = T_c$, while in the semi-infinite 2D Ising model with the surface field h_1 , the critical wetting transition takes place at $T = T_w$, $T_w < T_c$ [20]. Below, we discuss the properties of (5) and on this basis we define the characteristic temperatures $T_{w,M}^\gamma$ and $T_{c,M}^\gamma$.

First we consider $T < T_w$ case, for which $l = 2$, see (6). For small enough temperatures the left-hand side of (5) is an increasing function of ω , it equals 0 for $\omega = 0$, and thus this equation does not have a solution for $k = 1$ and $k = 2$. The coefficients ω_1 and ω_2 are thus found from (10) with $\alpha_1 = -1$ and $\alpha_2 = 1$. However, when T is getting close to T_w the situation becomes different: the left-hand side of (5) — upon increasing ω — first decreases, has a minimum and then increases. As a result (5) has a solution for $k = 2$. At the same time, to obtain coefficient ω_1 equation (10) must be used with $\alpha_1 = -1$. The M -dependent temperature, which separates the above two possibilities is denoted by $T_{w,M}^\gamma$.

When $T_w < T < T_c$, one has $l = 0$ and all coefficients ω_k are defined by (5).

For $T > T_c$, $l = 1$ and for temperatures well above T_c equation (5) does not have solution for $k = 1$; the coefficient ω_1 can be calculated from (10) with $\alpha_1 = +1$. When T is close to T_c the left-hand side of (5) is a non-monotonic function of ω , and thus the solution exists for any k . The characteristic temperature separating these two cases is denoted by $T_{c,M}^\gamma$.

Typical plots of the left-hand side of (5) are shown in figure 1.

To find the formulae for M -dependent temperatures $T_{w,M}^\gamma$ and $T_{c,M}^\gamma$ we use the fact that at these two temperatures (5) has double solution for $\omega = 0$. In other words, the condition

$$\left. \frac{\partial}{\partial \omega} \right|_{\omega=0} [(M+1)\omega - \delta'(\omega, T) - \phi(\omega, T, h_1)] = 0 \quad (13)$$

must be satisfied, which leads to

$$\frac{2W(T, h_1)}{W(T, h_1) - 1} - \frac{\sinh 2K}{\sinh(2K - 2K^*)} = M + 1, \quad (14)$$

where $W(T, h_1)$ is defined in (9). To find solutions of this equation it is useful to analyse its left-hand side as a function of temperature: it equals to 1 for $T = 0$, is an increasing function of temperature for $0 < T < T_w$, at $T = T_w$ reaches infinity and has a pole ($W = 1$ for $T = T_w$). For $T_w < T < T_c$ the left-hand side of (14) is negative and has another pole for $T = T_c$ ($K = K^*$ at $T = T_c$). For $T > T_c$ it decreases from infinity at

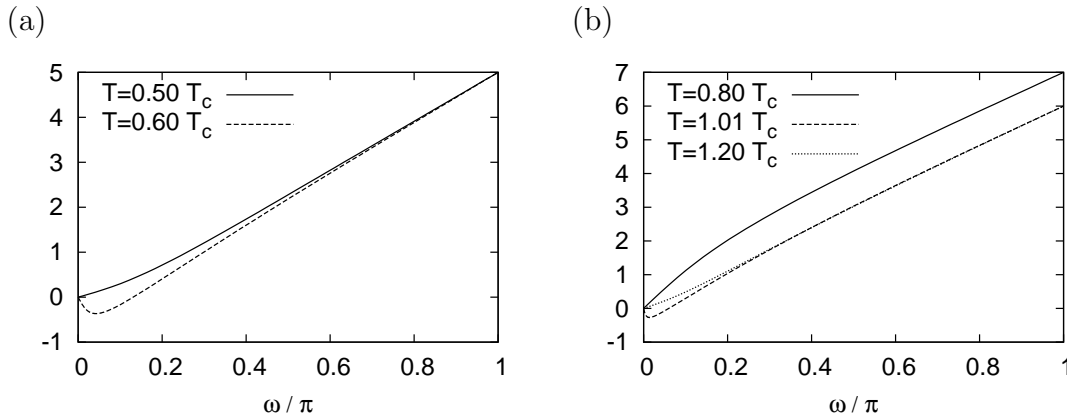


Figure 1. Plots of the left-hand side of (5) divided by π for $h_1 = 0.8J$ ($T_w \approx 0.621 T_c$) and $M = 5$. The solutions ω_k correspond to integer values of this function. For $T = 0.5T_c < T_{w,M}^\gamma$ there are $M - 1 = 4$ solutions, for $T_{w,M}^\gamma < T = 0.6T_c < T_w$ there are $M = 5$ solutions, for $T_w < T = 0.8T_c < T_c$ there are $M + 1 = 6$ solutions, for $T_c < T = 1.01T_c < T_{c,M}^\gamma$ there are $M + 1 = 6$ solutions, and for $T_{c,M}^\gamma < T = 1.2T_c$ there are $M = 5$ solutions. Total number of solutions is $M + 1 = 6$; the missing solutions correspond to imaginary values of ω and are determined from (10).

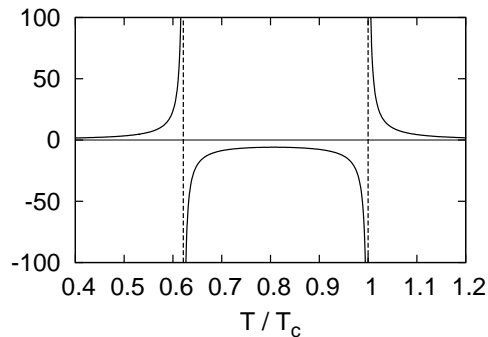


Figure 2. Plot of the left-hand side of (14) for $h_1 = 0.8J$ (for which $T_w \approx 0.621 T_c$). At pseudotransition temperatures $T_{w,M}^\gamma(h_1, M)$ and $T_{c,M}^\gamma(h_1, M)$ this function is equal to $M + 1$. To guide an eye the vertical broken lines corresponding to $T = T_w$ and $T = T_c$ are drawn.

$T = T_c$ to 0 for $T \rightarrow \infty$. A typical plot of left-hand side of (14) is shown in figure 2. Equation (14) has two solutions for any positive M – the solution $T_{w,M}^\gamma$ is always smaller than T_w and approaches the wetting temperature monotonically as $M \rightarrow \infty$, while the solution $T_{c,M}^\gamma(h_1, M)$ is always larger than T_c and decreases monotonically to T_c as $M \rightarrow \infty$.

3. Properties of pseudotransition temperatures

In an infinite strip of width M and dimension d larger than the lower critical dimension d_l , $d > d_l = 2$, true phase transitions corresponding to the non-analyticity of free energy

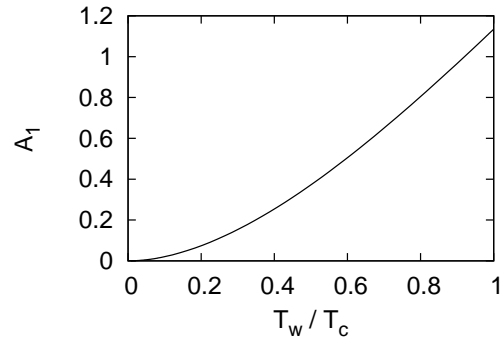


Figure 3. The plot of the amplitude A_1 (see (15)) as a function of T_w .

occur.

In a strip with symmetric surface fields (S) capillary condensation is expected. For a vanishing bulk field the strip is filled with phase favoured by the walls for $T < T_{c,M}$. The critical temperature $T_{c,M}$ is shifted away from T_c [27]. On the other hand, for antisymmetric surface fields (AS) with no bulk field, a transition is observed at $T_{w,M}$ that is shifted from T_w . For $T < T_{w,M}$ the interface separating two phases is located close to one of the walls while for $T > T_{w,M}$ this interface is located in the middle of the system [20]. Temperature $T_{w,M}$ approaches T_w as $M \rightarrow \infty$. In AS case the second phase transition at $T_{c,M}$ located close to T_c , also occurs.

In a two-dimensional strip no phase transition may occur for finite M . However, for large strip widths we expect some thermodynamics functions to vary rapidly close to certain temperature values while remaining analytic. It is convenient to define these pseudotransition temperatures which can be then used to characterise the behaviour of our system. Since all functions are analytic, these temperatures cannot be defined uniquely. There are different criteria according to which the pseudotransition temperature can be defined and thus there is no single $T_{w,M}$ and $T_{c,M}$. One possibility corresponds to $T_{w,M}^c$ and $T_{c,M}^c$ defined as the temperatures at which the specific heat attains its maximum values. Here we would like to show that the just defined temperatures $T_{w,M}^\gamma$ and $T_{c,M}^\gamma$ may be treated as such pseudotransition temperatures.

First we check how the difference $T_w - T_{w,M}^\gamma$ depends on the width of the strip M for large M . This can be done on the basis of (14). Using the implicit function theorem one obtains

$$\frac{T_w - T_{w,M}^\gamma}{T_c} = \frac{A_1(h_1)}{M} + O(M^{-2}), \quad A_1(h_1) = 2 \left(T_c \frac{\partial W}{\partial T} \Big|_{T=T_w} \right)^{-1}. \quad (15)$$

Figure 3 shows the plot of the amplitude $A_1(T_w)$ after reparametrization from h_1 to T_w has been done according to (8).

Parry and Evans [20] used scaling hypothesis to postulate that for $M \rightarrow \infty$

$$T_w - T_{w,M} \sim M^{-1/\beta_s}. \quad (16)$$

Because for a 2D Ising model $\beta_s = 1$ the behaviour of the difference between pseudotransition temperature $T_{w,M}^\gamma$ and T_w agrees with this hypothesis.

Similarly, for $T_{c,M}^\gamma$ one obtains from (14)

$$\frac{T_{c,M}^\gamma - T_c}{T_c} = \frac{A_2}{M} + \mathcal{O}(M^{-2}), \quad (17)$$

where the amplitude $A_2 = [2 \ln(1 + \sqrt{2})]^{-1}$ is universal. Since for a 2D Ising model one has $\nu = 1$, thus $(T_{c,M}^\gamma - T_c)/T_c \sim M^{-1/\nu}$ as expected on the basis of scaling arguments [21]. We note that $T_{c,M}^\gamma$ is always larger than T_c .

The wetting temperature is a continuous function of the surface field h_1 . Parry and Evans [20] proposed the scaling function X_{AS} which describes the dependence of $T_{w,M}$ on the width of the strip M and the surface field h_1 in the limit $h_1 \rightarrow 0$ and $M \rightarrow \infty$ with $h_1 M^{\Delta_1/\nu}$ fixed

$$\frac{T_c - T_{w,M}}{T_c} = M^{-1/\nu} X_{AS}(h_1 M^{\Delta_1/\nu}). \quad (18)$$

It turns out that the pseudocritical temperature $T_{w,M}^\gamma$ defined by (14) satisfies a similar scaling relation. We have found the exact expression for the corresponding scaling function X_{AS}^γ .

For a 2D Ising model $\Delta_1 = \frac{1}{2}$ and the scaled variable takes the form $x = h_1 M^{1/2}$. In order to find the scaling function $X_{AS}^\gamma(x)$

$$\frac{T_c - T_{w,M}^\gamma}{T_c} = M^{-1} X_{AS}^\gamma(x) + \mathcal{O}(M^{-2}), \quad (19)$$

we introduced in (14) the surface field $h_1 = x M^{-1/2}$ and obtained in the scaling limit

$$X_{AS}^\gamma(x) = [2 \ln(1 + \sqrt{2})]^{-1} + \frac{1}{4} (1 + \sqrt{2}) \ln(1 + \sqrt{2}) \left(\frac{x}{J}\right)^2. \quad (20)$$

It is interesting to note that this result is true only for fixed x ; the scaling function

$$X_{AS}^\gamma(x) = \lim_{M \rightarrow \infty} M \frac{T_c - T_{w,M}^\gamma(M, x M^{-1/2})}{T_c} \quad (21)$$

is not a uniform limit.

The scaling law (19) has finite size corrections of order M^{-2} which are present even for $h_1 = 0$.

4. Solvation forces

4.1. Definition

The free energy of the strip per column can be calculated from (2) and (3). For both S and AS cases it naturally decomposes into the sum of three terms

$$\bar{f}^\alpha(T, h_1, M) = M f_b(T) + f_s^\alpha(T, h_1) + f_{\text{int}}^\alpha(T, h_1, M), \quad (22)$$

where $\alpha \in \{\text{S}, \text{AS}\}$, f_b is the bulk free energy density [28] equal to

$$f_b(T) = -k_B T \left[\frac{1}{2\pi} \int_0^\pi \operatorname{arccosh} [\cosh(2K - 2K^*) + 1 - \cos \omega] d\omega + \frac{1}{2} \ln(2 \sinh 2K) \right], \quad (23)$$

$f_s^\alpha(T, h_1)$ is the surface free energy per column, and the remaining term $f_{\text{int}}^\alpha(T, h_1, M)$ describes the interaction between the boundaries of the strip per column. By definition, the surface free energy $f_s^\alpha(T, h_1)$ does not depend on M , and $f_{\text{int}}^\alpha(T, h_1, M)$ tends to 0 as $M \rightarrow \infty$.

In general, the solvation force is defined as minus derivative of f_{int}^α with respect to the distance between the boundary walls. In the present case, because M is integer, we use the definition

$$f_{\text{solv}}^\alpha(T, h_1, M) = -[f_{\text{int}}^\alpha(T, h_1, M+1) - f_{\text{int}}^\alpha(T, h_1, M)] / k_B T, \quad (24)$$

where the factor $1/k_B T$ is additionally introduced to make the solvation force dimensionless. This definition is equivalent to

$$f_{\text{solv}}^\alpha(T, h_1, M) = [\bar{f}^\alpha(T, h_1, M) - \bar{f}^\alpha(T, h_1, M+1) + f_b(T)] / k_B T. \quad (25)$$

It is also useful to introduce the difference between the solvation forces corresponding to different boundary fields configurations

$$\Delta f_{\text{solv}}(T, h_1, M) = f_{\text{solv}}^{\text{AS}}(T, h_1, M) - f_{\text{solv}}^{\text{S}}(T, h_1, M). \quad (26)$$

Using (2), (3) and (25) it is straightforward to show that

$$\Delta f_{\text{solv}}(T, h_1, M) = \gamma_1(T, h_1, M) - \gamma_1(T, h_1, M+1). \quad (27)$$

This difference is easier to study analytically than the expression for $f_{\text{solv}}^\alpha(T, h_1, M)$, see (25).

4.2. Basic properties

We start our analysis by evaluating numerically the solvation forces for different temperatures T , strip widths M and surface fields h_1 .

In the symmetric case (S) the solvation force is always negative (attractive). For h_1 close to J this force has a minimum at $T_{\text{min}}^{\text{S} >} > T_c$ and tends to 0 both in the small and large temperature limits. Upon decreasing the boundary field h_1 , the absolute value of solvation force decreases, and for h_1 small enough a second minimum appears at $T_{\text{min}}^{\text{S} <} < T_c$. Upon further decreasing h_1 , the minimum located at $T_{\text{min}}^{\text{S} >}$ disappears. The range of h_1 for which $f_{\text{solv}}^{\text{S}}$ has two minima depends on M , and for $M \rightarrow \infty$ this range shrinks to 0. Plots of the solvation force in the symmetric case as a function of temperature for different boundary fields are presented in figure 4. The behaviour of this force will be studied in detail using scaling functions later on.

In the antisymmetric case (AS) the solvation force is plotted in figure 5. For $h_1 = J$ this force is positive (repulsive) for all temperatures and has maximum at $T_{\text{max}}^{\text{AS}}$ located

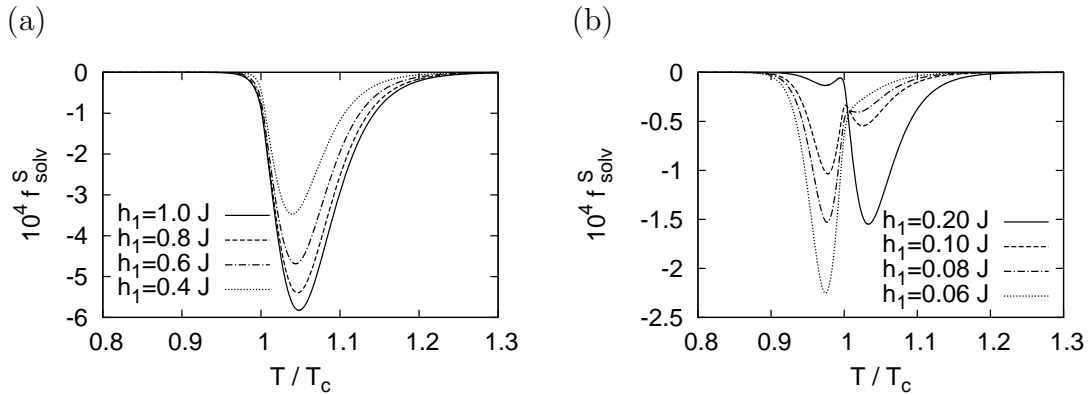


Figure 4. Plots of the solvation force in the symmetric case ($h_1 = h_2$) as a function of temperature for $M = 25$ and different values of the boundary field h_1 .

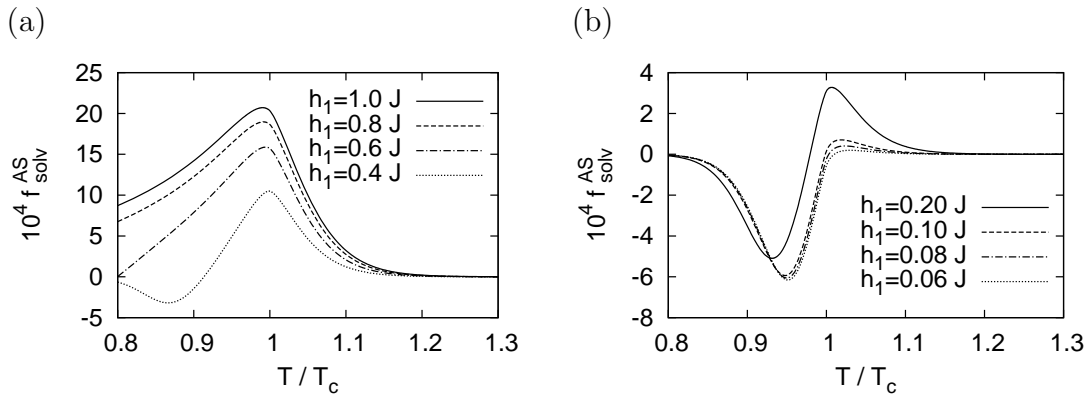


Figure 5. Plots of the solvation force in the antisymmetric case ($h_2 = -h_1$) as a function of temperature for $M = 25$ and different values of the boundary field h_1 .

slightly below T_c . The solvation force $f_{\text{solv}}^{\text{AS}}(T, h_1 = J, M)$ tends to 0 in the high and low temperature limits. However, for $h_1 < J$ the solvation force changes sign. It is negative for small temperatures, has a minimum at $T_{\text{min}}^{\text{AS}} < T_w$, and zero at T^* slightly above T_w . For temperatures higher than T^* the solvation force is positive and has a maximum close to T_c . For h_1 approaching 0, T^* tends to T_c and the (negative) value at the minimum below the wetting temperature decreases. The (positive) maximum value of the solvation force also decreases and disappears in the limit $h_1 \rightarrow 0$. We also looked at the location of the maximum of the solvation force $T_{\text{max}}^{\text{AS}}$. For small M , $T_{\text{max}}^{\text{AS}}$ is located above T_c . Upon increasing M the temperature $T_{\text{max}}^{\text{AS}}$ first crosses the critical temperature and then, upon further increasing of M , approaches T_c from below. The exact value of M at which $T_{\text{max}}^{\text{AS}}$ is equal to T_c depends on the boundary field h_1 . We note that the limiting value of the solvation force at $h_1 = 0$ is the same for both boundary fields configurations. Some of the above described properties of solvation force have been reported for a different system in [9].

The leading M -dependence of the solvation force evaluated at T_c is known exactly [29, 30]

$$f_{\text{solv}}^{\text{S}}(T_c, h_1, M) = -\frac{\pi}{48M^2} + \mathcal{O}(1/M^3), \quad (28a)$$

$$f_{\text{solv}}^{\text{AS}}(T_c, h_1, M) = \frac{23\pi}{48M^2} + \mathcal{O}(1/M^3), \quad (28b)$$

$$f_{\text{solv}}^{\text{O}}(T_c, 0, M) = -\frac{\pi}{48M^2} + \mathcal{O}(1/M^3). \quad (28c)$$

The above values of the universal amplitudes are also recovered numerically in our analysis.

We checked numerically that for $T \neq T_c$ [31]

$$f_{\text{solv}}^{\text{S}}(T, h_1, M) \sim \exp[-M/\xi_b(T)], \quad (29)$$

where [32]

$$\xi_b = \begin{cases} (4K - 4K^*)^{-1} & \text{for } T < T_c, \\ (2K^* - 2K)^{-1} & \text{for } T > T_c \end{cases} \quad (30)$$

is the bulk correlation length. Using (27) and the dependence of γ_1 on M for fixed T [26] we checked that (29) implies the following leading order decay of the solvation force in the antisymmetric case

$$f_{\text{solv}}^{\text{AS}}(T, h_1, M) \sim \begin{cases} \exp[-M \ln W(T, h_1)] & \text{for } T < T_w, \\ \exp[-M/\xi_b(T)] & \text{for } T = T_w, \\ 1/M^3 & \text{for } T_w < T < T_c, \\ 1/M^2 & \text{for } T = T_c, \\ \exp[-M/\xi_b(T)] & \text{for } T > T_c. \end{cases} \quad (31)$$

The solvation force is a continuous function of temperature and the above formula is correct only in the $M \rightarrow \infty$ limit. Below we discuss the behaviour of the solvation force around T_w and T_c by introducing the appropriate scaling functions.

4.3. Scaling at T_w

To study properties of the solvation force close to T_w in the antisymmetric case we take the scaling limit $M \rightarrow \infty$, $T \rightarrow T_w$ with parameter $X = M \ln W(T, h_1) \sim (T_w - T)M$ fixed. The function $W(T, h_1)$ has been introduced in the scaling variable to simplify the scaling function.

To study the solvation force in this limit we use (27). For $T < T_w$ coefficient γ_1 is given by (10) with $k = 1$ and $\alpha_1 = -1$

$$e^{-uM} = e^{i\delta'(iu, T)} \frac{W(T, h_1, M) e^{-u} (e^{-u} - W(T, h_1, M)^{-1})}{e^{-u} - W(T, h_1, M)}, \quad (32)$$

where the solution u gives γ_1 using (4) with $\omega_1 = iu$.

We put $M = X/\ln W$ in (32) and calculate the limit $T \rightarrow T_w$ using l'Hôpital's rule. After introducing $H(X) = \frac{\partial}{\partial W} u(W, X)|_{W=1}$ one gets

$$e^{-XH(X)} = \frac{H(X) - 1}{H(X) + 1}, \quad H(X) < 0. \quad (33)$$

The function $H(X)$ can be calculated numerically for any $X > 0$. The solution of (32) in the scaling limit takes the following form

$$u = H(X) \ln W + O(\ln^2 W), \quad (34)$$

and one obtains[‡]

$$\gamma_1(X, h_1, M) = \nu(h_1) - \frac{1}{M^2} \frac{X^2 H^2(X)}{2 \sinh \nu(h_1)} + O\left(\frac{1}{M^3}\right), \quad (35)$$

where $\nu(h_1) = (2K - 2K^*)|_{T=T_w(h_1)}$.

Comparison of this result with (29) leads to the conclusion that the first term on the right-hand side of (26) dominates in the scaling regime (except of $T = T_w$) and the second term may be neglected.

With the help of (35) one gets

$$f_{\text{solv}}^{\text{AS}}(X, h_1, M) = -\frac{1}{M^3} G(X, h_1) + O\left(\frac{1}{M^4}\right), \quad (36)$$

where

$$G(X, h_1) = \frac{X^3 H^2(X)}{\sinh \nu(h_1)} \frac{H^2(X) - 1}{2 + X(H^2(X) - 1)}. \quad (37)$$

Using (33) and (37) it is straightforward to analyse the properties of the scaling function $G(X, h_1)$. For small X

$$G(X, h_1) = \frac{X}{\sinh \nu} + O(X^2), \quad (38)$$

it has a maximum at $X_0 \approx 3.22149$ and approaches zero exponentially for large X , see figure 6.

The above properties can be used to explain the behaviour of the solvation force around the wetting temperature for large M . In particular, one has

$$\frac{T_w - T_{\text{min}}^{\text{AS}}}{T_c} = \frac{A_3(h_1)}{M} + O\left(\frac{1}{M^2}\right), \quad (39)$$

$$f_{\text{solv}}^{\text{AS}}(T_{\text{min}}^{\text{AS}}, h_1, M) = -\frac{A_4(h_1)}{M^3} + O\left(\frac{1}{M^4}\right), \quad (40)$$

where the functions $A_3(h_1)$ and $A_4(h_1)$ are positive and may be obtained from the scaling function G and the definition of scaling variable X .

The dependence of T^* on M can be explained using (26). Exactly at $T = T_w$ the left-hand side of this equation is zero (exactly at T_w the coefficient $\gamma_1(T, h_1, M)$ does

[‡] Note that the expression (35) for the function $\gamma_1(X, h_1, M)$ is not equivalent to equation (4.7) in [24], because of an error in calculation.

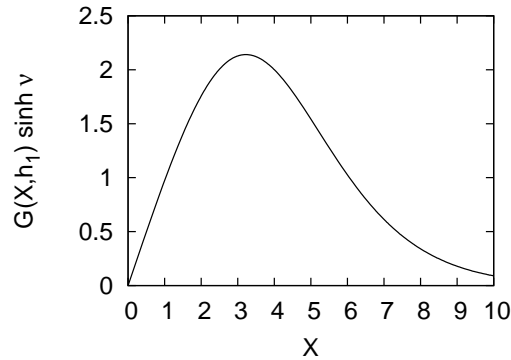


Figure 6. The scaling function $G(X, h_1)$ for the solvation force in the antisymmetric case multiplied by $\sinh \nu(h_1)$ (see (36)).

not depend on M) so the solvation force is the same for both AS and S boundary fields. With the help of equations (27), (29) and (38) one gets

$$\frac{T^* - T_w}{T_c} = A_5(h_1) M^2 \exp[-M/\xi_b(T_w(h_1))], \quad (41)$$

where $A_5(h_1)$ is a positive function.

4.4. Scaling at T_c

For temperatures close to the bulk critical temperature the solvation force takes in the limit $T \rightarrow T_c$, $M \rightarrow \infty$ with fixed h_1 and $\bar{x} = \text{sign}(T - T_c) M/\xi_b(T)$, the following scaling form

$$f_{\text{solv}}^\alpha(T, h_1, M) = \frac{1}{M^2} \mathcal{X}_{h_1}^\alpha(\bar{x}) + O(M^{-3}). \quad (42)$$

Note that the factor $\text{sign}(T - T_c)$ introduced in the definition of the scaling variable \bar{x} makes it negative for $T < T_c$ and positive for $T > T_c$. The bulk correlation length (30) close to T_c takes the form

$$\xi_b(T) \approx \begin{cases} \xi_0^+ |t|^{-1} & \text{for } T > T_c \ (x > 0), \\ \xi_0^- |t|^{-1} & \text{for } T < T_c \ (x < 0), \end{cases} \quad (43)$$

where $t = (T - T_c)/T_c$ and the amplitudes $\xi_0^+ = 2\xi_0^- = 1/[2 \ln(1 + \sqrt{2})]$, such that $\bar{x} \sim (T - T_c) M$ for T close to T_c . Later on we will use

$$x = tM/\xi_0^+ \approx \begin{cases} \bar{x} & \text{for } \bar{x} > 0, \\ \bar{x}/2 & \text{for } \bar{x} < 0, \end{cases} \quad (44)$$

instead of the scaling variable \bar{x} .

The scaling function \mathcal{X} has already been proposed by Evans and Stecki [31] and has been calculated analytically in both S and AS cases for particular value of the scaling field $h_1 = J$. Here we consider arbitrary values of h_1 . Our numerical calculations show that, up to numerical errors,

$$\mathcal{X}_{h_1}^\alpha(x) = \mathcal{X}_J^\alpha(x) \quad \text{for } h_1 \neq 0. \quad (45)$$

We have found numerically that the corrections to scaling depend on h_1 and are getting smaller for h_1 close to J . Unfortunately, we are unable to prove analytically this property of scaling function $\mathcal{X}_{h_1}^\alpha(x)$.

However, the difference between the scaling functions for the two cases

$$\Delta\mathcal{X}_{h_1}(x) = \mathcal{X}_{h_1}^{\text{AS}}(x) - \mathcal{X}_{h_1}^{\text{S}}(x) \quad (46)$$

can be calculated exactly. For T close to T_c this function is obtained from (27), (4), (5) and (6). To derive ω_1 in the scaling limit we replace M with $x\xi_0^+/t$ in (5) and use the following property of the function $\phi(\omega, T, h_1)$

$$\lim_{T \rightarrow T_c} \phi(\omega_1(T, h_1, M), T, h_1) = 0 \quad (47)$$

for $h_1 \neq 0$. Thus the only term that depends on the surface field in (5) disappears in this scaling limit and the calculation of $\Delta\mathcal{X}$ goes along the same lines as in [31] (from now on we drop the index h_1 in $\Delta\mathcal{X}$). This is in full agreement with (45). One obtains

$$\Delta\mathcal{X} = \frac{w^2 \sin w}{w - \sin w \cos w}, \quad (48)$$

with w being a solution of

$$w \cot w = x, \quad (49)$$

where $0 \leq w < \pi$ for $x \leq 1$, and $w = iu$, $u > 0$ for $x > 1$.

Function $\mathcal{X}_{h_1}^{\text{S}}(x)$ for different h_1 -values is plotted in figure 7a. Note that such obtained curves are indistinguishable from each other which numerically proves (45) for the symmetric case. It has a minimum for $x > 0$, so from (42) it follows that for large M

$$T_{\min}^{\text{S}}(h_1, M) = T_c \left[1 + \frac{A_6}{M} + O(M^{-2}) \right], \quad (50)$$

$$f_{\text{solv}}^{\text{S}}(T_{\min}^{\text{S}}, h_1, M) = -\frac{A_7}{M^2} + O(M^{-3}), \quad (51)$$

with A_6 and A_7 determined by the position of minimum of the scaling function

$$A_6 \approx 1.26424, \quad A_7 \approx 0.43052. \quad (52)$$

Because $\mathcal{X}_{h_1}^{\text{S}}(x)$ has only one minimum, the second minimum of the solvation force, located below T_c , disappears in this limit.

Function $\mathcal{X}_{h_1}^{\text{AS}}(x)$ for different h_1 -values is plotted in figure 7b. Again one notes that such obtained curves are indistinguishable from each other which numerically proves (45) for the antisymmetric case. It has a maximum for $x < 0$ and from (42) it follows that for large M

$$T_{\max}^{\text{AS}}(h_1, M) = T_c \left[1 - \frac{A_8}{M} + O(M^{-2}) \right], \quad (53)$$

$$f_{\text{solv}}^{\text{AS}}(T_{\max}^{\text{AS}}, h_1, M) = \frac{A_9}{M^2} + O(M^{-3}), \quad (54)$$

with A_8 and A_9 determined by the position of maximum of the scaling function

$$A_8 \approx 0.2651, \quad A_9 \approx 1.5341. \quad (55)$$

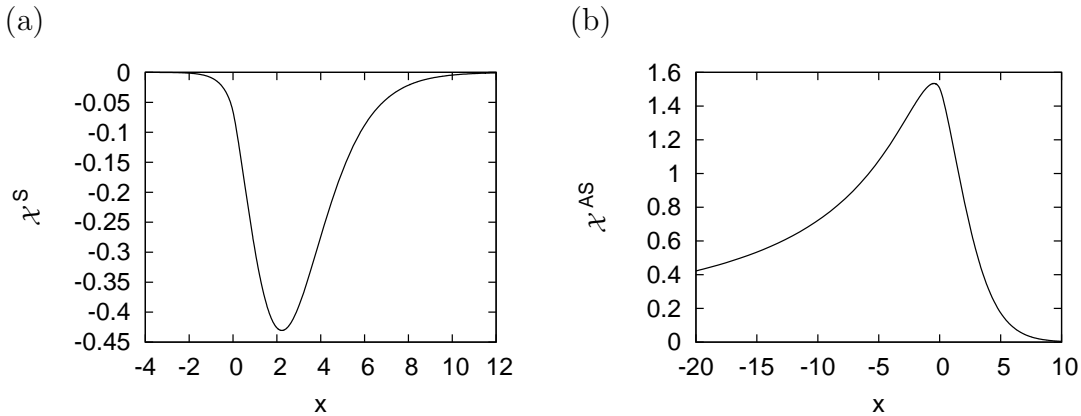


Figure 7. The scaling function \mathcal{X} describing the solvation force for any $h_1 \neq 0$ and $M \rightarrow \infty$ with $x = tM/\xi_0^+$ fixed for: (a) symmetric ($h_1 = h_2$), and (b) antisymmetric ($h_1 = -h_2$) boundary fields. Each plot does not depend on the chosen value of h_1 and is the same (up to numerical errors smaller than the resolution of the plot) as the analytically calculated scaling functions for $h_1 = J$ [31].

The temperature T_{\max}^{AS} is smaller than T_c in this limit. These results have already been reported in [31] for $h_1 = J$. According to our numerical analysis the values of constants A_6, A_7, A_8 and A_9 are the same for any nonzero surface field h_1 . §

4.5. Scaling for $T_w \rightarrow T_c$

To explain the properties of the solvation force for small values of the boundary field h_1 we consider the scaling limit $M \rightarrow \infty$, $T \rightarrow T_c$ and $h_1 \rightarrow 0$ (i.e. $T_w \rightarrow T_c$) with two scaling variables

$$x = \frac{tM}{\xi_0^+}, \quad y = \frac{A_0}{k_B T_c} \frac{h_1}{|t|^{1/2}} \quad (56)$$

fixed. In this limit the solvation force can be described by scaling function $\mathcal{Y}^\alpha(x, y)$

$$f_{\text{solv}}^\alpha(T, h_1, M) = \frac{1}{M^2} \mathcal{Y}^\alpha(x, y) + O(M^{-3}). \quad (57)$$

The constant $A_0 = [(1 + \sqrt{2}) / \ln(1 + \sqrt{2})]^{1/2}$ in (56) was chosen such that for negative values of x , the value $y = 1$ corresponds to $T = T_w$. For $y < 1$ equation (57) gives the solvation force for T below T_w , and for $y > 1$ – for T above T_w . This scaling function has already been analysed for subcritical temperatures in [18].||

The scaling function $\mathcal{Y}^\alpha(x, y)$ can only be calculated numerically; details of evaluation are presented in Appendix A.

§ Note a minor disagreement between values of our numerical amplitudes A_8 and A_9 (55) and those evaluated in [31] due to minor numerical inaccuracies in [31].

|| There is a mistake in the scale of variable x in figures 3, 4 and 5 in [18]. To get the correct values of x one should replace x by $(\xi_0^-)^{-2} x$ in these figures in [18].

Table 1. The rules for picking the correct solutions of (60) corresponding to γ_1 . In all four cases there exists exactly one solution for a given range of w .

Range of x and y	Domain of w	Condition on w
$y > 1, x \leq (y^2 - 1) / (y^2 + 1)$	real	$0 \leq w < \min \left\{ \pi, x (y^4 - 1)^{1/2} \right\}$
$y > 1, x > (y^2 - 1) / (y^2 + 1)$	imaginary	$0 < w/i < x (y^2 + 1) (1 + 2y^2)^{-1/2}$
$y \leq 1, x > 0$	imaginary	$x (1 - y^4)^{1/2} < w/i$
$y \leq 1, x \leq 0$	imaginary	$w/i < x (y^2 + 1) (1 + 2y^2)^{-1/2}$ $ x (1 - y^2) \leq w/i \leq x (1 - y^4)^{1/2}$

Before presenting the numerically evaluated properties of the scaling functions $\mathcal{Y}^\alpha(x, y)$, $\alpha = S, AS$ we note that one can test some of these properties through analytically determined difference

$$\Delta\mathcal{Y}(x, y) = \mathcal{Y}^{AS}(x, y) - \mathcal{Y}^S(x, y). \quad (58)$$

This can be done with the help of (27). The coefficient γ_1 is given by equation (5), where its solution ω_1 determines γ_1 by (4). After applying the scaling limit to the above equation one gets

$$\gamma_1(T, h_1, M) = \frac{1}{M} \sqrt{x^2 + w^2} + O(M^{-2}), \quad (59)$$

where w is a solution of

$$w \cot w = x \frac{x^2 [y^2 + \text{sign}(x)]^2 + w^2 [1 + 2\text{sign}(x) y^2]}{x^2 (y^4 - 1) - w^2}. \quad (60)$$

Depending on x and y equation (60) may have many different solutions for w . The rules for choosing the correct solution are summarised in table 1; other solutions give the coefficients γ_k for $k > 1$.

The function $\Delta\mathcal{Y}$ is given by the formula

$$\Delta\mathcal{Y}(x, y) = - \lim_{M \rightarrow \infty} M^2 \left(\frac{\partial \gamma_1}{\partial M} \right)_{T, h_1}, \quad (61)$$

which leads to a rather lengthy expression and we refrain from presenting it here.

The scaling functions $\mathcal{Y}^\alpha(x, y)$ are plotted in figure 8. These plots cannot be used directly to approximate the behaviour of the solvation force as a function of temperature for large fixed M , because for fixed y both the temperature T and the surface field h_1 become functions of x . Additionally, the limit $x \rightarrow 0$ corresponds to $h_1 \rightarrow 0$, which explains why — for any y — one has

$$\mathcal{Y}^{AS}(0, y) = \mathcal{Y}^S(0, y) = -\frac{\pi}{48}, \quad (62)$$

i.e. in this limit the scaling function equals the universal amplitude describing the decay of the solvation force at $T = T_c$ for free boundary conditions.

To explain the observed properties of solvation force we changed variables in the scaling function and defined new function

$$\tilde{\mathcal{Y}}^\alpha(x, z) = \mathcal{Y}^\alpha \left(x, \sqrt{z/|x|} \right), \quad (63)$$

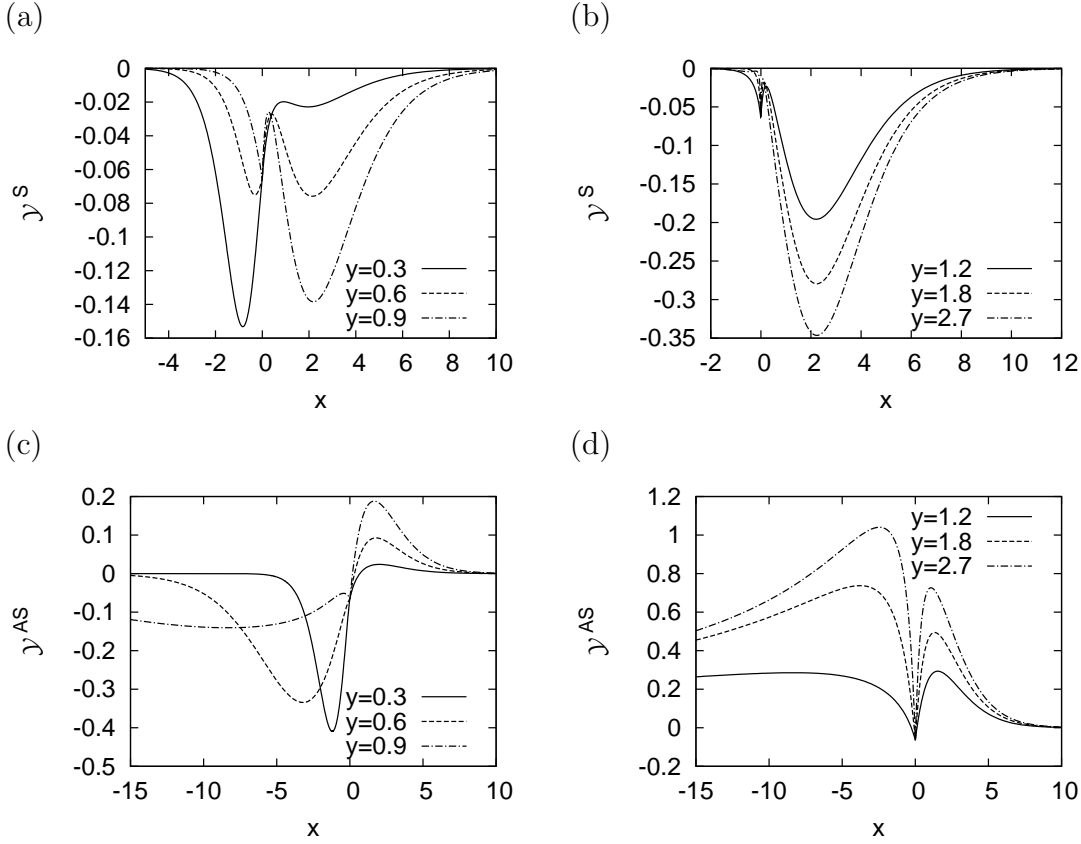


Figure 8. The scaling function $\mathcal{Y}^\alpha(x, y)$ as function of x for different values of y . Boundary fields are symmetric ($\alpha = S$) in graphs (a) and (b), and antisymmetric ($\alpha = AS$) in graphs (c) and (d).

where the new variable $z = |x|y^2 \sim Mh_1^2$, so that fixing x and z is equivalent to fixing x and y in the scaling limit. For the new scaling variables one obtains

$$f_{\text{solv}}^\alpha(T, h_1, M) = \frac{1}{M^2} \tilde{\mathcal{Y}}^\alpha(x, z) + O(1/M^3), \quad (64)$$

which can be used to approximate the solvation force as a function of temperature for fixed M and h_1 . Plots of $\tilde{\mathcal{Y}}$ are presented in figure 9.

We checked that up to our numerical precision

$$\lim_{z \rightarrow \infty} \tilde{\mathcal{Y}}^\alpha(x, z) = \mathcal{X}^\alpha(x), \quad \lim_{z \rightarrow 0} \tilde{\mathcal{Y}}^\alpha(x, z) = \mathcal{X}^0(x), \quad (65)$$

which is not surprising since for $M \rightarrow \infty$ and fixed $h_1 \neq 0$ one has $z \sim Mh_1^2 \rightarrow \infty$, while $h_1 = 0$ implies $z = 0$.

In both S and AS cases the scaling functions $\tilde{\mathcal{Y}}^\alpha(x, y)$ reflect the behaviour of solvation force for small surface fields. For symmetric surface fields, the negative function $\tilde{\mathcal{Y}}^S(x, z)$ has for fixed $z < z_1 \approx 0.1474$ only one minimum at negative values of x . At $z = z_1$ the second minimum located at positive x appears. Upon further increasing of z , the minimum at $x < 0$ is increasing and the absolute value of the second minimum

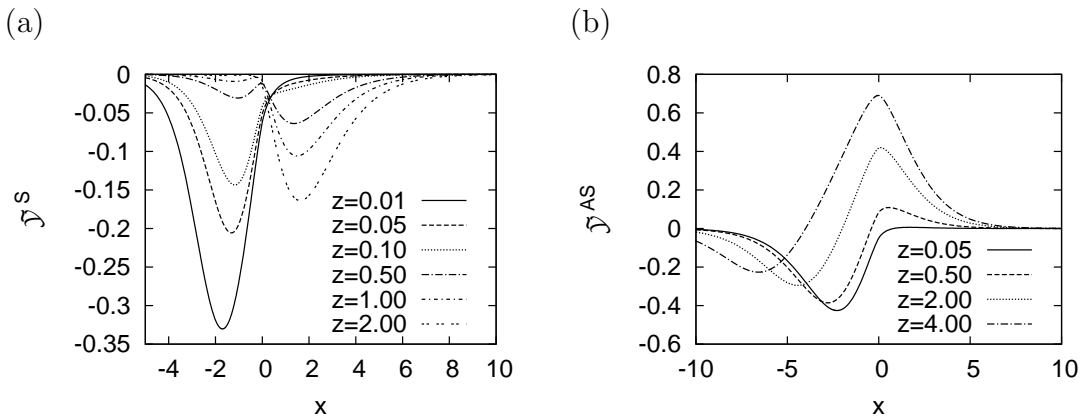


Figure 9. The scaling function $\tilde{\mathcal{Y}}^\alpha(x, y)$ for fixed z as a function of x . Boundary fields are symmetric ($\alpha = S$) in graph (a) and antisymmetric ($\alpha = AS$) in graph (b).

is increasing. We could not observe the disappearance of the minimum at negative x , because for large z the depth of this minimum is of order of our numerical errors.

For antisymmetric surface fields the scaling function $\tilde{\mathcal{Y}}^{AS}(x, z)$ has exactly one minimum and one maximum for all finite z . The minimum is always located at $x < 0$ and moves towards $-\infty$ when z is increased. The maximum moves from $x = \infty$ for $z = 0$ to a finite negative value of x for $z = \infty$. The value of scaling function at maximum is always positive and becomes very small for z close to 0. For $z = z_2 \approx 0.212$ the scaling function vanishes at $x = 0$, which means that (up to higher order corrections) the solvation force disappears at $T = T_c$. On the other hand, at $z = z_3 \approx 3.35$, the maximum of scaling function is located exactly at $x = 0$.

The above observations are summed up below:

- in the S case the minimum of the solvation force located above T_c exists for

$$h_1/J > \frac{A_{10}}{\sqrt{M}} + O(M^{-3/2}), \quad A_{10} \approx 0.40, \quad (66)$$

- in the AS case the solvation force is zero at $T = T_c$ for

$$h_1/J = \frac{A_{11}}{\sqrt{M}} + O(M^{-3/2}), \quad A_{11} \approx 0.48, \quad (67)$$

- in the AS case the maximum of the solvation force is located exactly at $T = T_c$ for

$$h_1/J = \frac{A_{12}}{\sqrt{M}} + O(M^{-3/2}), \quad A_{12} \approx 1.89. \quad (68)$$

Finally, we study the behaviour of the solvation force at $T = T_c$

$$f_{\text{solv}}^\alpha(T_c, h_1, M) = \frac{\mathcal{A}^\alpha(z)}{M^2} + O(M^{-3}). \quad (69)$$

The amplitude $\mathcal{A}^\alpha(z)$ can be calculated using the scaling function

$$\mathcal{A}^\alpha(z) = \tilde{\mathcal{Y}}^\alpha(x=0, z). \quad (70)$$

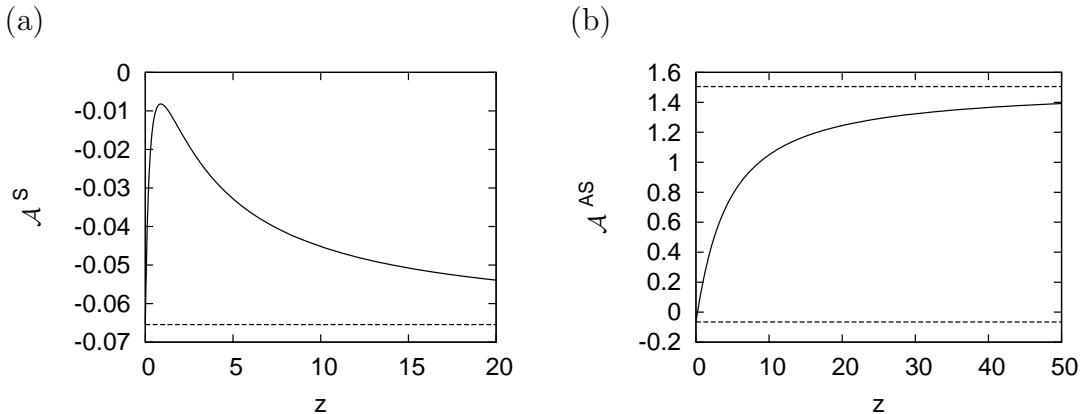


Figure 10. The amplitudes $\mathcal{A}^\alpha(z)$ describing the decay of the solvation force at $T = T_c$ for $M \rightarrow \infty$ (see (69)); (a) symmetric surface fields, (b) antisymmetric surface fields. Dashed lines show the exactly known values of amplitudes for $z = 0$ and $z \rightarrow \infty$.

From (28a), (28b) and (28c) the values of the amplitudes $\mathcal{A}^\alpha(z)$ for $z = 0$ and $z \rightarrow \infty$ follow

$$\mathcal{A}^S(z=0) = \mathcal{A}^{AS}(z=0) = \mathcal{A}^S(z=\infty) = -\frac{\pi}{48}, \quad \mathcal{A}^{AS}(z=\infty) = \frac{23\pi}{48}. \quad (71)$$

For other values of z amplitudes $\mathcal{A}^\alpha(z)$ can be calculated numerically; they are presented in figure 10.

5. Summary

In this article we considered the two-dimensional Ising strip of width M with surface fields h_1 and h_2 acting on the boundaries of the system. We considered only symmetric ($h_1 = h_2$) and antisymmetric ($h_1 = -h_2$) configurations of the surface fields.

We introduced two pseudotransition temperatures: $T_{w,M}^\gamma$ and $T_{c,M}^\gamma$. Around $T_{w,M}^\gamma$, in the antisymmetric case, the interface separating two magnetic phases moves from position close to one wall to the centre of the strip. At $T_{c,M}^\gamma$ the difference between the two phases disappears. The existence of these two temperatures follows from the properties of our solution for the free energy. We proved that $T_{w,M}^\gamma$ and $T_{c,M}^\gamma$ have the same scaling properties as real transition temperatures in higher dimensions. We also checked scaling relations of $T_{w,M}^\gamma$ postulated by Parry and Evans [20].

The major part of our analysis was concentrated on the properties of the solvation force. We calculated this force as a function of temperature T , surface field h_1 and strip width M . For symmetric surface fields this force is always negative (attractive). For strong surface fields the solvation force has a minimum above the bulk critical temperature of the 2D system T_c , while for small surface fields the minimum is located below T_c . There exists a range of surface fields for which this force has two minima. For antisymmetric surface fields (and $h_1 \neq J$) the solvation force changes the sign: it is negative for small temperatures and positive (repulsive) for high temperatures. The

temperature T^* at which the solvation force is zero is located very close to the wetting temperature of the semi-infinite system T_w . For large surface fields the solvation force has a maximum below T_c . When the surface field is decreased, this maximum crosses T_c . Upon further decrease of h_1 the maximum disappears.

To explain these properties we proposed scaling functions in three different scaling regimes: at T_w , at T_c , and in the case when $T_w \rightarrow T_c$.

For antisymmetric surface fields close to T_w we found scaling in the limit $M \rightarrow \infty$ and $T \rightarrow T_w$ with $M(T - T_w)$ fixed. We succeeded in finding the analytical formula for the scaling function and used it to explain the behaviour of the solvation force. The scaling function is nonuniversal, i.e. it depends on the magnitude of surface field.

Close to T_c the scaling limit is $M \rightarrow \infty$ and $T \rightarrow T_c$ with $M(T - T_c)$ fixed. For both symmetric and antisymmetric surface fields the obtained scaling function is, within our numerical accuracy, independent of h_1 for $h_1 \neq 0$. We also showed analytically that the difference between scaling functions in both configurations of surface fields is independent of h_1 . Using properties of such obtained scaling functions we explained the location of maxima and minima of the solvation force around T_c for strong surface fields.

The third scaling limit corresponds to $h_1 \rightarrow 0$, which implies $T_w \rightarrow T_c$, $T \rightarrow T_c$ and $M \rightarrow \infty$ with $M(T - T_c)$ and Mh_1^2 fixed. In this limit we calculated the scaling function numerically and checked that it explains the location of minima and maxima of the solvation force for small surface fields.

Acknowledgments

Helpful discussions with A. Maciołek, D. Danchev, S. Dietrich, O. Vasilyev, and F. Toldin are gratefully acknowledged.

Appendix A. Numerical calculation of scaling function $\mathcal{Y}^\alpha(x, y)$

In this appendix we explain methods used to calculate the scaling functions. From (56) and (57) we get the formula

$$\mathcal{Y}^\alpha(x, y) = \lim_{M \rightarrow \infty} \mathcal{Y}_M^\alpha(x, y), \quad \mathcal{Y}_M^\alpha(x, y) = M^2 f_{\text{sol}}^\alpha(T(x, M), h_1(x, y, M), M), \quad (\text{A.1})$$

where $T(x, M) = T_c(1 + x\xi_0^+/M)$ and $h_1(x, y, M) = yk_B T_c/A_0(x\xi_0^+/M)^{1/2}$. Function $\mathcal{Y}_M^\alpha(x, y)$ can be calculated numerically with arbitrary numerical precision. However, when M is large or high precision is required, the time spend on calculation becomes very long. Although the limiting value $\mathcal{Y}^\alpha(x, y)$ cannot be calculated exactly, it may be estimated in several ways. One possibility is to fix a large but finite M and assume

$$\mathcal{Y}^\alpha(x, y) \approx \mathcal{Y}_M^\alpha(x, y). \quad (\text{A.2})$$

This method was used in [18] with $M = 200$.

In this paper we applied the least squares method. Because the difference $\mathcal{Y}^\alpha(x, y) - \mathcal{Y}_M^\alpha(x, y)$ depends on M and its absolute values are large for small M , this method cannot be used directly.

To overcome this problem and to estimate the value of $\mathcal{Y}^\alpha(x, y)$ we calculate the values of $\mathcal{Y}_M^\alpha(x, y)$ for $M = M_0, M_0 + 1, M_0 + 2, \dots, M_0 + m$ and fit the results to the formula

$$\mathcal{Y}_M^\alpha(x, y) = B_0 + \frac{B_1}{M} + \frac{B_2}{M^2} + \dots + \frac{B_n}{M^n}, \quad (\text{A.3})$$

which we assume to reflect the form of leading corrections to the scaling. We take B_0 as our estimate of $\mathcal{Y}^\alpha(x, y)$. The accuracy of this algorithm depends on values of parameters M_0 , m and n . The larger values used the more accurate the result is; we used $M_0 = 190$, $m = 10$ and $n = 3$.

The accuracy of such obtained results may be estimated by comparing them with the results obtained for different values of M_0 . In addition, to test our results we used (58) with $\Delta\mathcal{Y}$ calculated analytically. The obtained relative accuracy is better than 10^{-4} .

References

- [1] Fisher M E and de Gennes P G 1978 *C.R. Acad. Ser. B* **287** 207
- [2] Christenson H K and Blom C E 1987 *J. Chem. Phys.* **86** 419
- [3] Evans R 1990 *J. Phys.: Condens. Matter* **2** 8989
- [4] Burkhardt T W and Eisenriegler E 1995 *Phys. Rev. Lett.* **74** 3189
- [5] Danchev D 1996 *Phys. Rev. E* **53** 2104
- [6] Hanke A, Schlesener F, Eisenriegler E and Dietrich S 1998 *Phys. Rev. Lett.* **81** 1885
- [7] Garcia R and Chan M H W 1999 *Phys. Rev. Lett.* **83** 1187
- [8] Kardar M and Golestanian R 1999 *Rev. Mod. Phys.* **71** 1233
- [9] Maciołek A, Drzewiński A and Bryk P 2004 *J. Chem. Phys.* **120** 1921
- [10] Dantchev D and Krech M 2004 *Phys. Rev. E* **69** 046119
- [11] Fukuto M, Yano Y F and Pershan P S 2005 *Phys. Rev. Lett.* **94** 135702
- [12] Ganshin A, Scheidemantel S, Garcia R and Chan M H W 2006 *Phys. Rev. Lett.* **97** 075301
- [13] Rafai S, Bonna D and Meunier J 2007 *Physica A* **386** 31
- [14] Schmidt F M and Diehl H W 2008 *Phys. Rev. Lett.* **101** 100601
- [15] Soyka F, Zvyagolskaya O, Hertlein C, Helden L and Bechinger C 2008 *Phys. Rev. Lett.* **101** 208301
- [16] Hertlein C, Helden L, Gambassi A, Dietrich S and Bechinger C 2008 *Nature* **451** 172
- [17] Tröndle M, Harnau L, and Dietrich S 2008 *J. Chem. Phys.* **129** 124716
- [18] Nowakowski P and Napiórkowski M 2008 *Phys. Rev. E* **78** 060602
- [19] Krech M 1994 *The Casimir effect in critical systems* (Singapore: World Scientific)
- [20] Parry A O and Evans R 1992 *Physica A* **181** 250, 1990 *Phys. Rev. Lett.* **64** 439
- [21] Barber M N 1983 Finite-size scaling *Phase Transitions and Critical phenomena* vol 8, ed C Domb and J L Lebowitz (New York: Academic)
- [22] Kaufman B 1949 *Phys. Rev.* **76** 1232
- [23] Abraham D B and Martin-Löf 1973 *Commun. Math. Phys.* **32** 245
- [24] Stecki J, Maciołek A and Olaussen K 1993 *Phys. Rev. B* **49** 1092
- [25] Kramers H A and Wannier G H 1941 *Phys. Rev.* **60** 252
- [26] Maciołek A and Stecki J 1996 *Phys. Rev. B* **54** 1128
- [27] Evans R, Marini Bettolo Marconi U and Tarazona P 1986 *J. Chem. Phys.* **84** 2376
- [28] Onsager L 1944 *Phys. Rev.* **65** 117

- [29] Cardy J L 1986 *Nucl. Phys. B* **275** 200
- [30] Nightingale and M P Indekeu J O 1985 *Phys. Rev. Lett.* **54** 1824; Blöte H W J, Cardy J L and Nightingale M P 1986 *Phys. Rev. Lett.* **56** 742
- [31] Evans R and Stecki J 1994 *Phys. Rev. B* **49** 8842
- [32] Palmer J 2007 Planar Ising correlations *Prog. Math. Phys.* **49** (Boston: Birkhäuser)